Supporting information

Surface Chemistry Mediates the Tumor Entrance of Nanoparticles Probed by Single-Molecule Dual-Imaging Nanodots

Huiming Ren,[a] Qiuhui Hu,[a,b] Yuji Sun,[a] Xiaoxuan Zhou,[b] Yincong Zhu,[a] Qiuyang Dong,[a] Linying Chen,[a] Jianbin Tang,[a] Hongjie Hu,[b] Youqing Shen[a] and Zhuxian Zhou[a,]*

[a]Key Laboratory of Biomass Chemical Engineering of Ministry of Education and Zhejiang Key Laboratory of Smart Biomaterials, College of Chemical and Biological Engineering, Zhejiang University, Hangzhou 310027, China

[b]Department of Radiology, Sir Run Run Shaw Hospital (SRRSH) of School of Medicine, Zhejiang University, Hangzhou, Zhejiang, 310027, China

*Correspondence: zhouzx@zju.edu.cn

1. Supplemental Figures and Tables....3
Scheme S1. Synthesis procedure of **PDI-16Fmoc-G2.5**. 3
Scheme S2. Synthesis procedure of **PDI-16DOTA(tBu)-G3**. 4
Scheme S3. Synthesis procedure of **G6-Ac**. 5
Figure S1. ^{1}H NMR spectrum of Fmoc-Lys-Boc-OPFP in $CDCl_3$. 5
Figure S2. ^{1}H NMR spectrum of PDI-16Fmoc-G2.5 in DMSO-d_6. 6
Figure S3. ^{1}H NMR spectrum of Fmoc-Lys-Fmoc-OPFP in $CDCl_3$. 6
Figure S4. ^{1}H NMR spectra of PDI-16DOTA(tBu)-Gn (n = 3-6) in DMSO-d_6. 7
Figure S5. MALDI-TOF mass spectrum of PDI-16DOTA(tBu)-G3. 7
Figure S6. Hydrodynamic size distribution of Gn-Ac (n = 4-6) measured by dynamic light scattering (DLS). 8
Figure S7. TEM image of G6-Ac positively stained with 2% aqueous sodium phosphotungstate. ×120 k, 80 kV, scale bar = 100 nm. 8
Figure S8. The comparison of the zeta potential between dendrimer with and without Gd. 8
Figure S9. Plots of $1/T_1$ versus the concentration of the contrast agents at 3T. 9
Figure S10. The dorsal whole-body fluorescence imaging of mice with 4T1 breast cancer cells of the PDI-16(DOTA-Gd) PLL dendrimers. 9
Figure S11. The abdomen fluorescence imaging of the mice with 4T1 breast cancer cells of the PDI-16(DOTA-Gd) PLL dendrimers. 10
Figure S12. (a) The whole body T1-weighted MR images of mice bearing 4T1 orthotopic tumor before (pre) and after post-injection of ProHance®, G6-Ac and G6-OEG, at 0.1 mmol-Gd/kg. MRI signals enhancement ratio (ER = Spost /Spre) of artery **(b)**, kidneys **(c)** and liver **(d)**. 10
Figure S13. (a) The experimental procedure for determining the cellular take and exocytosis of the nanodots on 4T1 cells. (b) The flow cytometry of 4T1 cells treated with different nanodots (10 μM) for 24 h. (c) The flow cytometry of 4T1 cells with nanodots exocytosed in fresh medium for another 24 h. 11
Figure S14. Confocal laser scanning microscopy (CLSM) images and the cellular uptake of 4T1 cells after 12 h incubation with 20 μM of the nanoprobes (Scale bar = 15 μm). 11
Table S1. Molecular weights of PDI-DOTA PLL dendrimers determined by Maldi-Tof. 12
Table S2. Molecular weights of PDI-DOTA PLL dendrimers determined by GPC. 12
Table S3. The parameters of the linear fitting in **Figure S6**. 13

1. Supplemental Figures and Tables

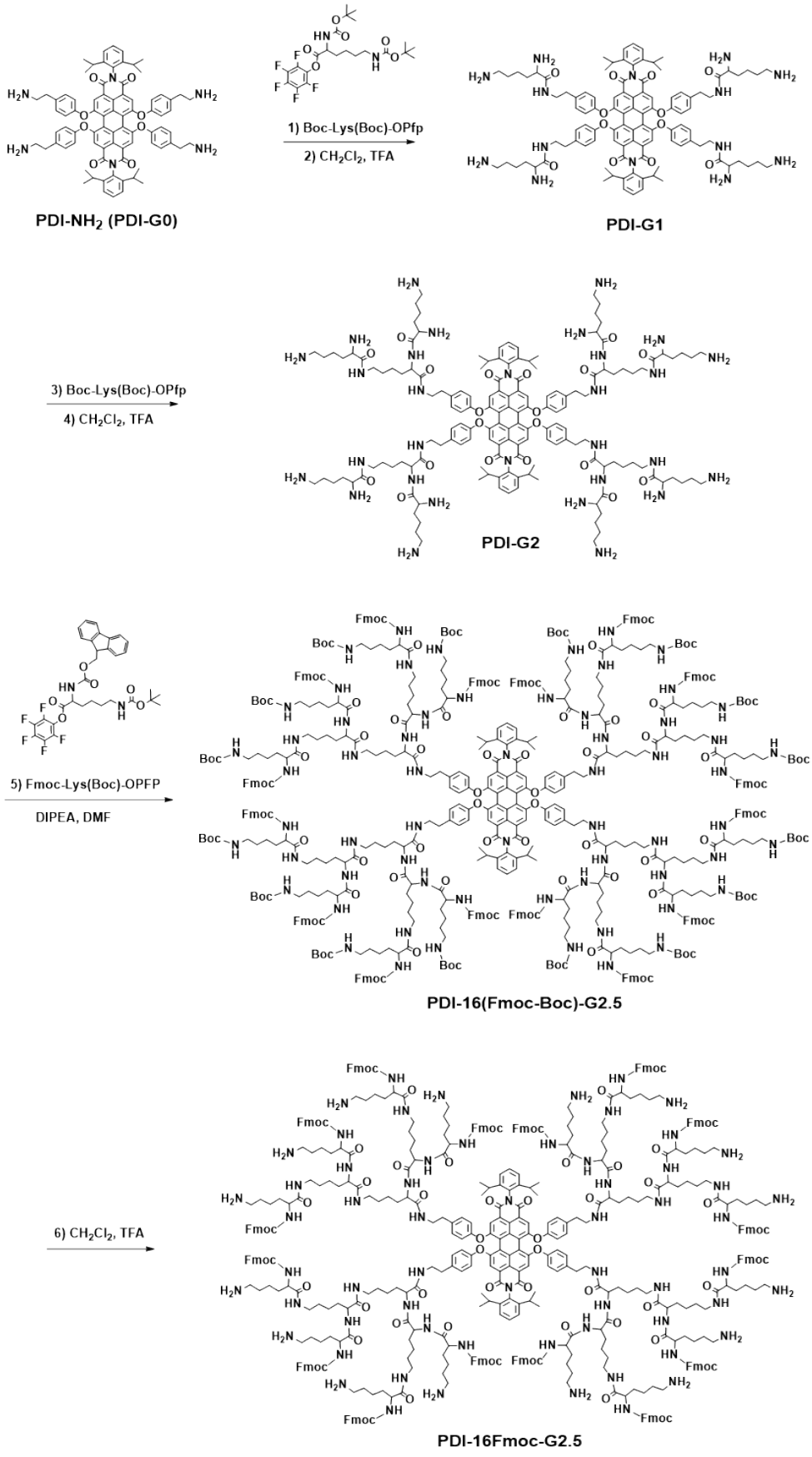

Scheme S1. Synthesis procedure of **PDI-16Fmoc-G2.5**.

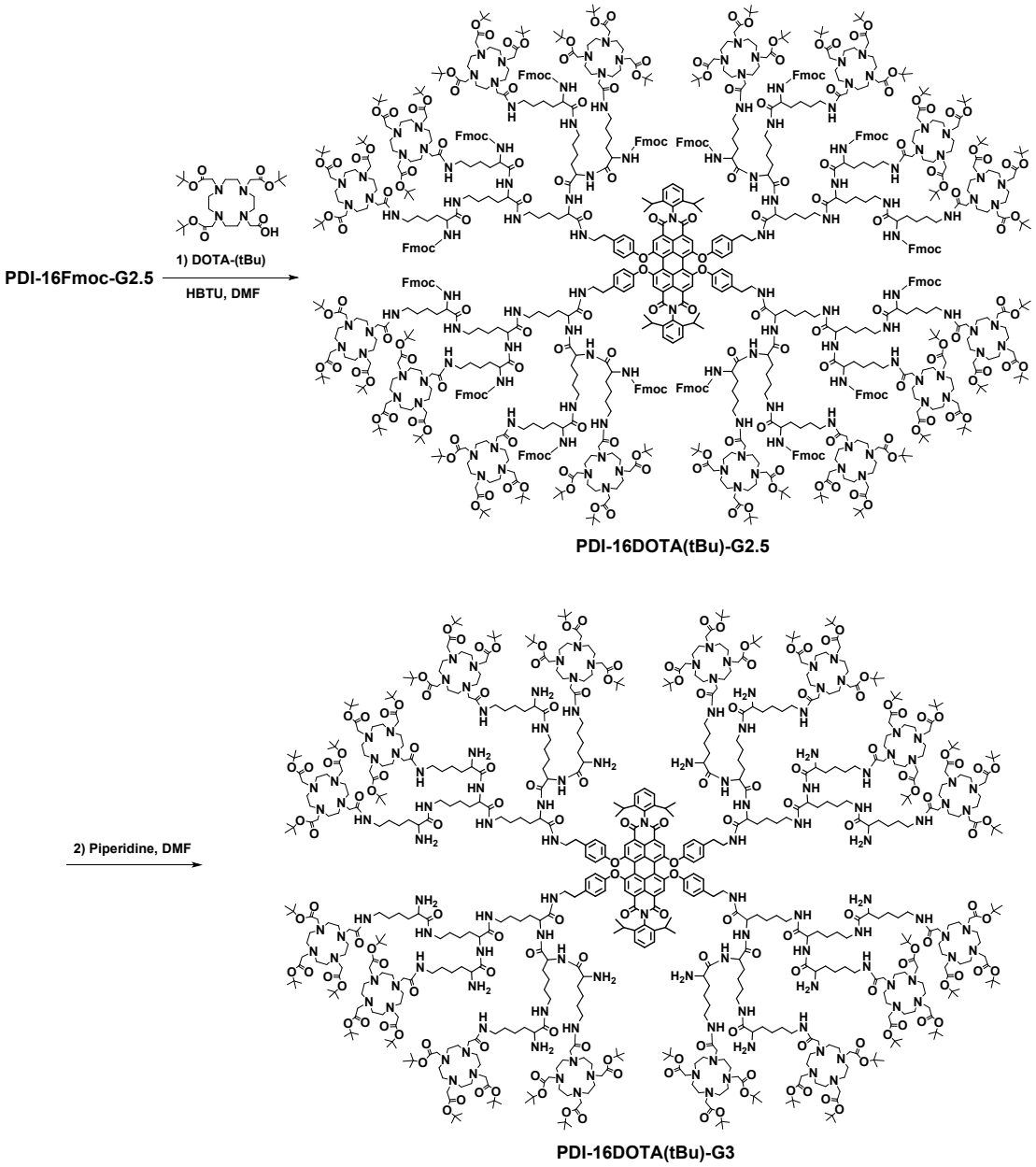

Scheme S2. Synthesis procedure of **PDI-16DOTA(tBu)-G3**.

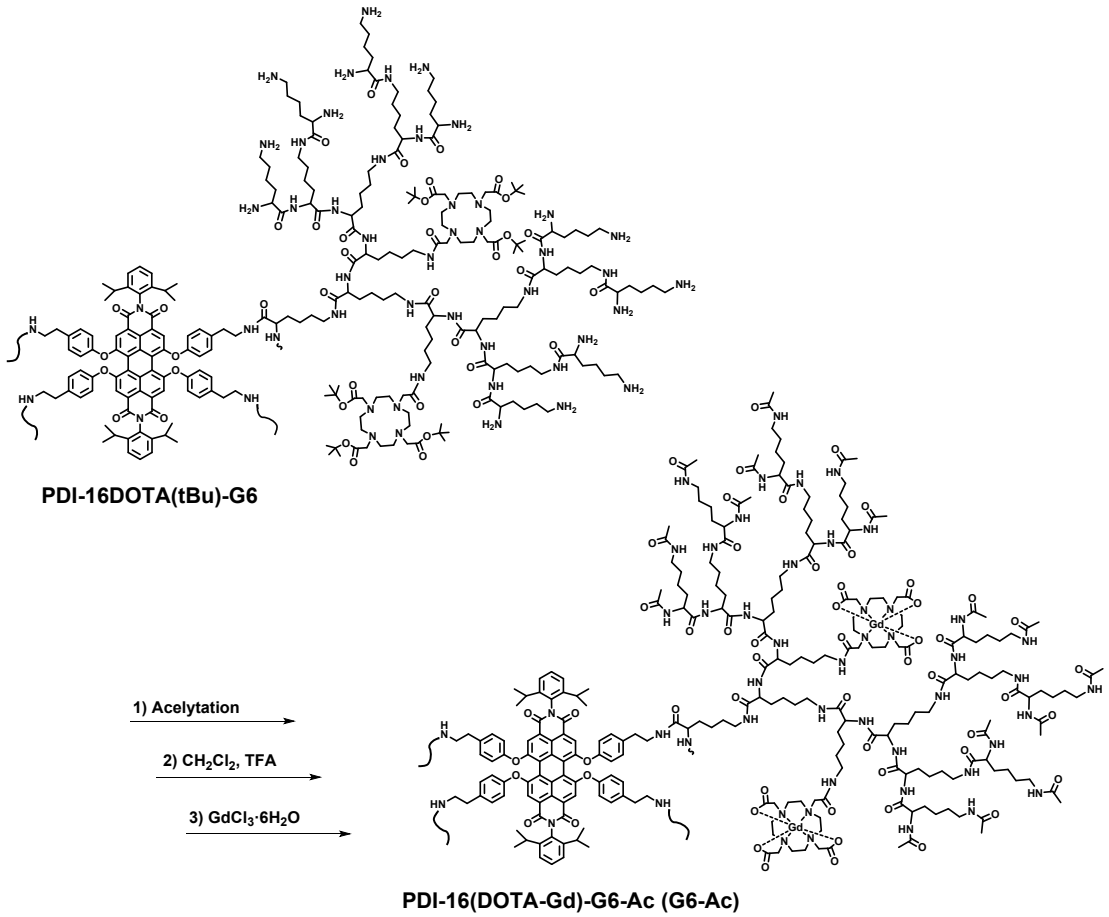

Scheme S3. Synthesis procedure of **G6-Ac**.

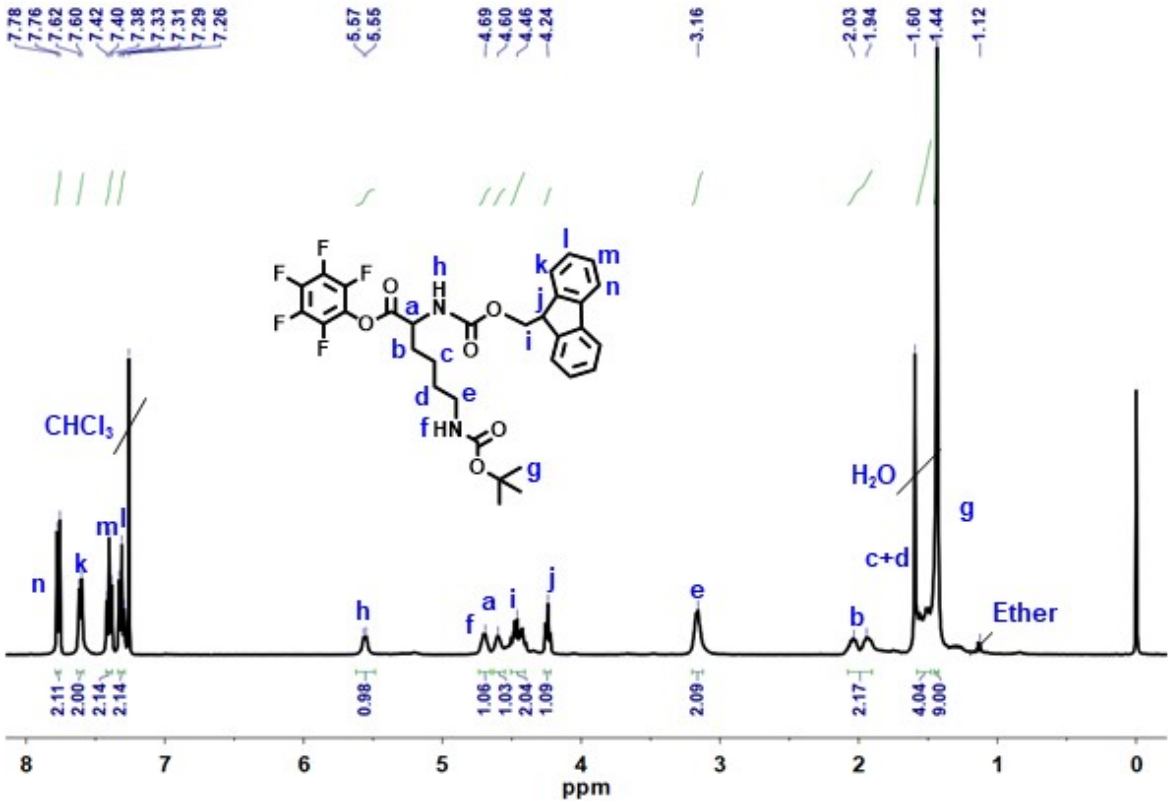

Figure S1. ^{1}H NMR spectrum of Fmoc-Lys-Boc-OPFP in $CDCl_3$.

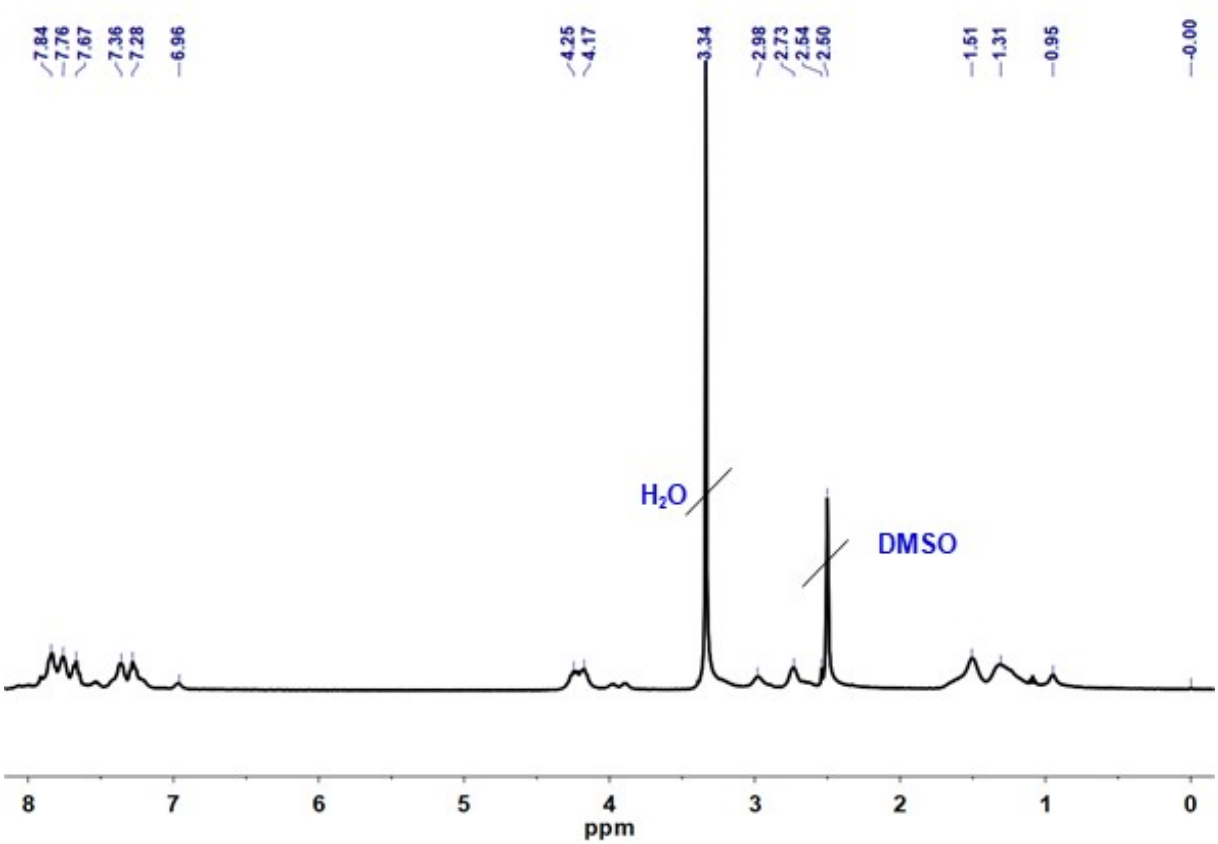

Figure S2. ^{1}H NMR spectrum of PDI-16Fmoc-G2.5 in DMSO-d_6.

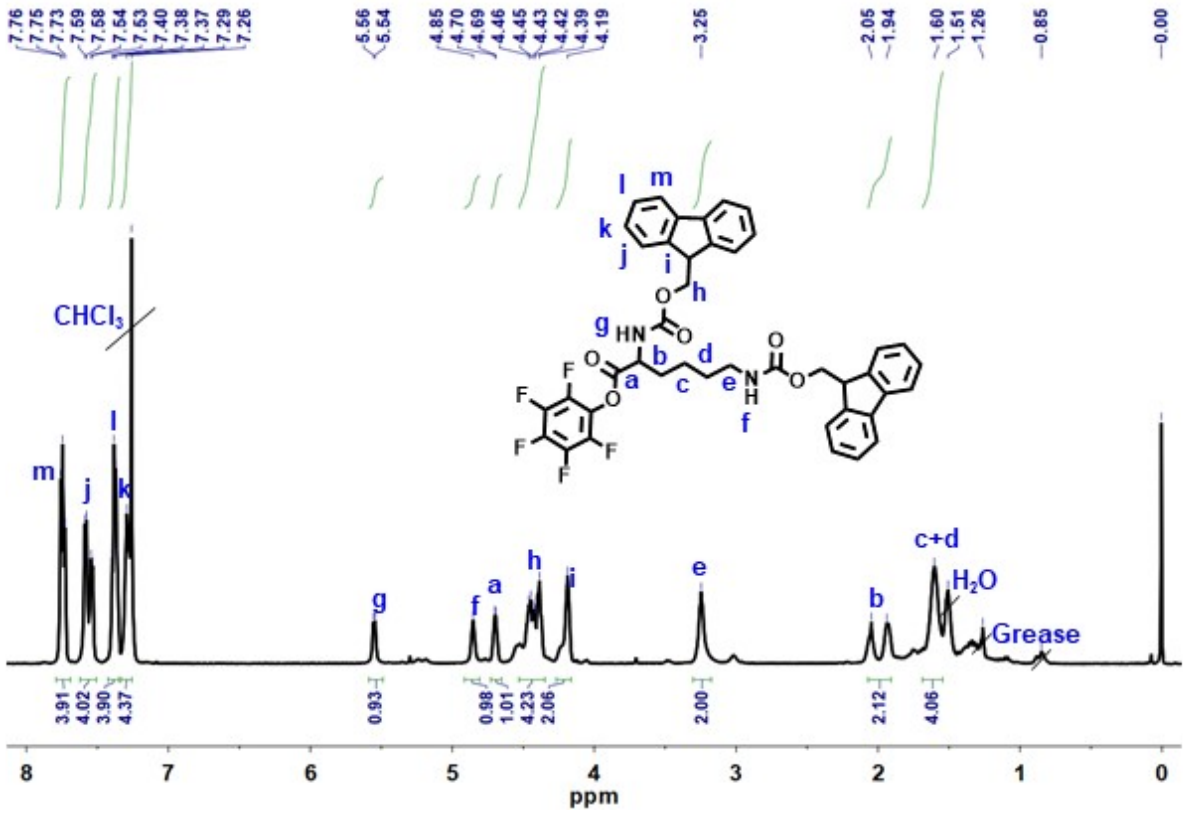

Figure S3. ^{1}H NMR spectrum of Fmoc-Lys-Fmoc-OPFP in $CDCl_3$.

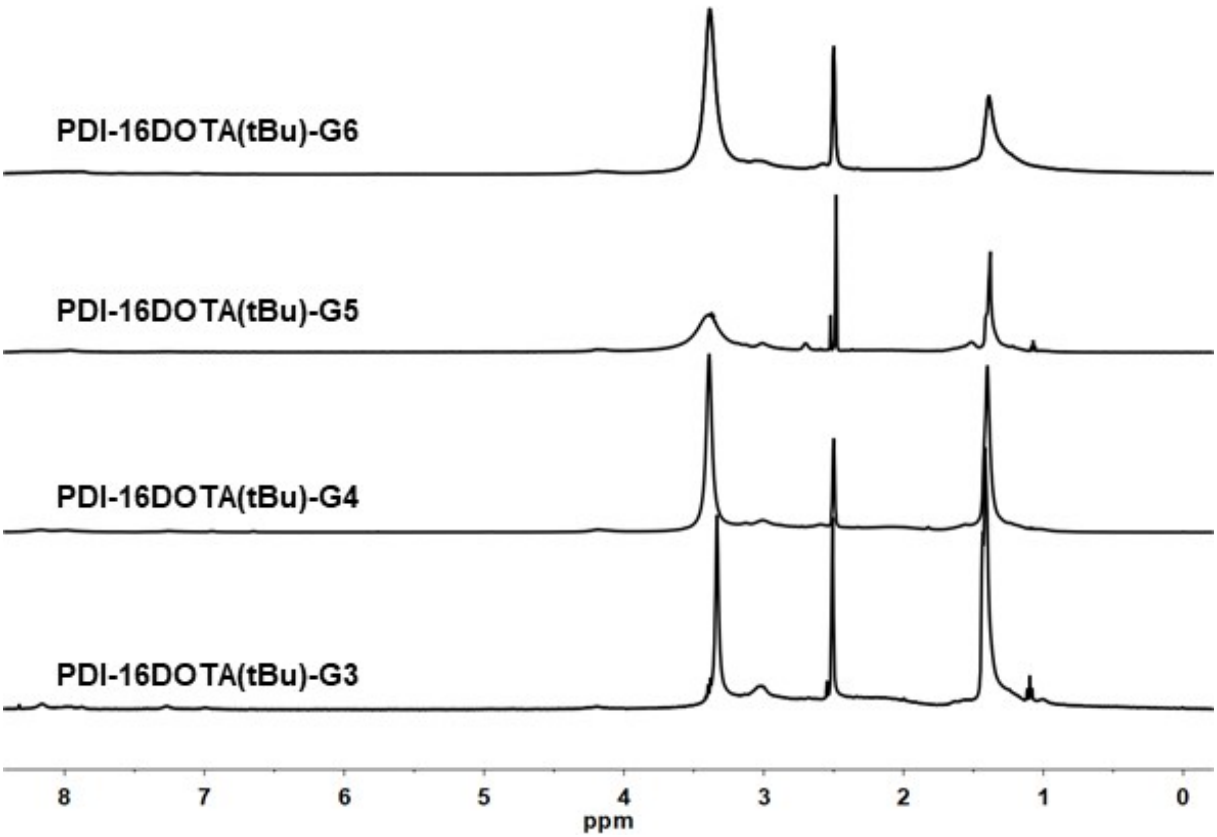

Figure S4. ^{1}H NMR spectra of PDI-16DOTA(tBu)-Gn (n = 3-6) in DMSO-d_6.

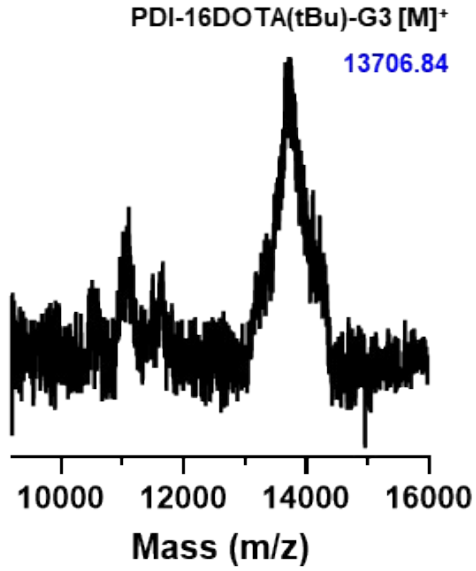

Figure S5. MALDI-TOF mass spectrum of PDI-16DOTA(tBu)-G3.

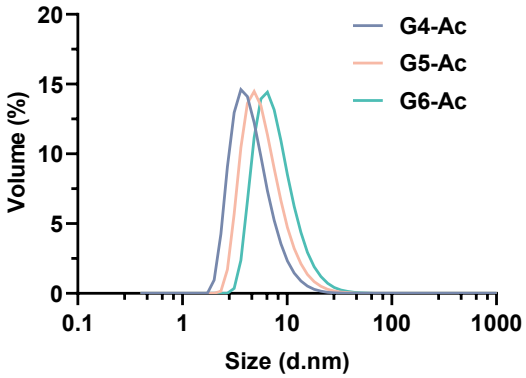

Figure S6. Hydrodynamic size distribution of Gn-Ac (n = 4-6) measured by dynamic light scattering (DLS).

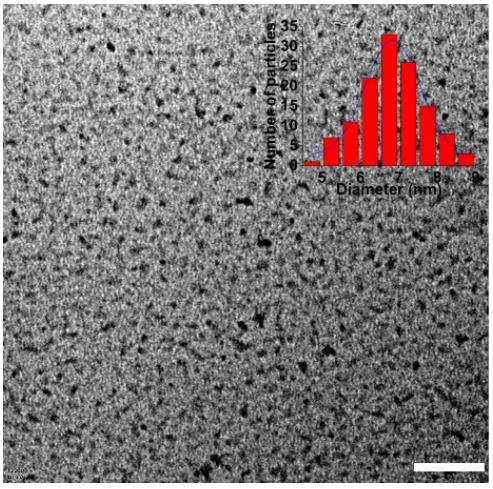

Figure S7. TEM image of G6-Ac positively stained with 2% aqueous sodium phosphotungstate. ×120 k, 80 kV, scale bar = 100 nm.

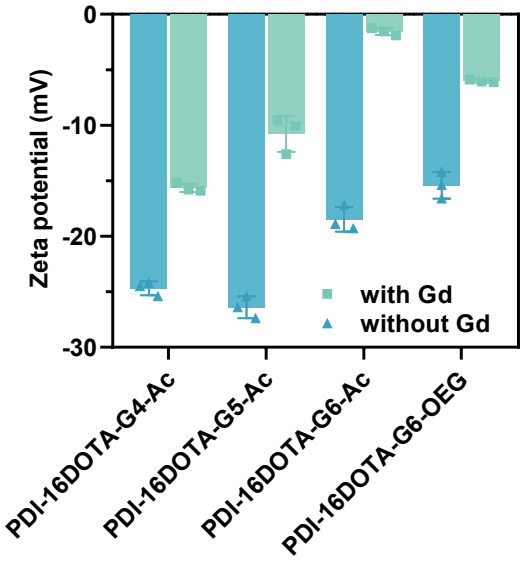

Figure S8. The comparison of the zeta potential between dendrimer with and without Gd.

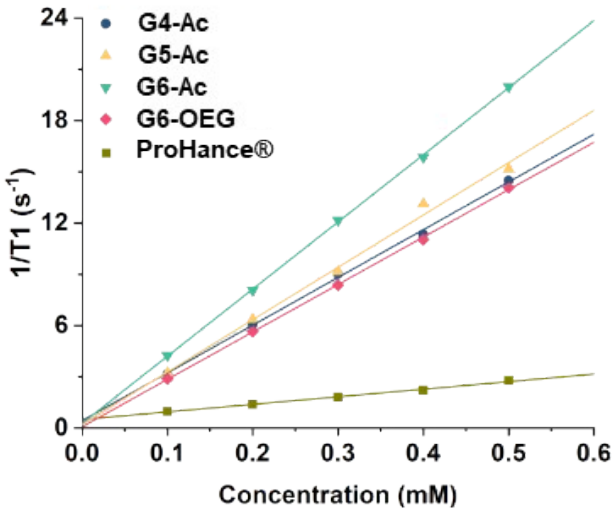

Figure S9. Plots of $1/T_1$ versus the concentration of the contrast agents at 3T.

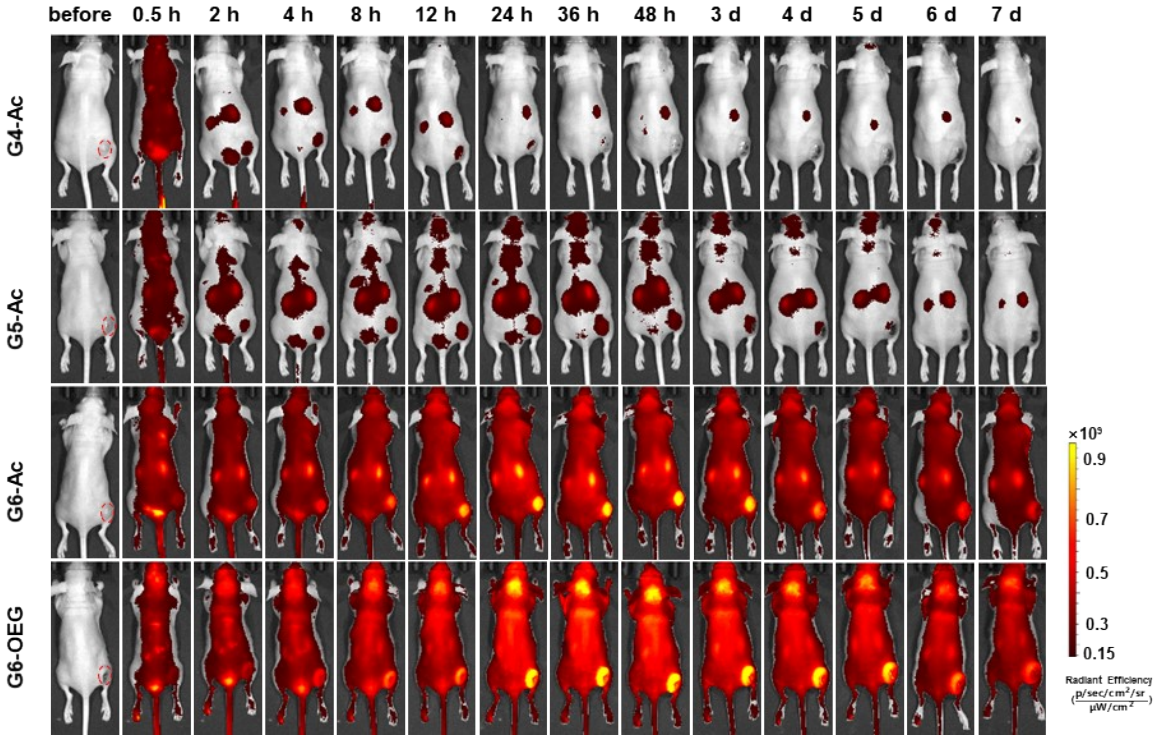

Figure S10. The dorsal whole-body fluorescence imaging of mice with 4T1 breast cancer cells of the PDI-16(DOTA-Gd) PLL dendrimers.

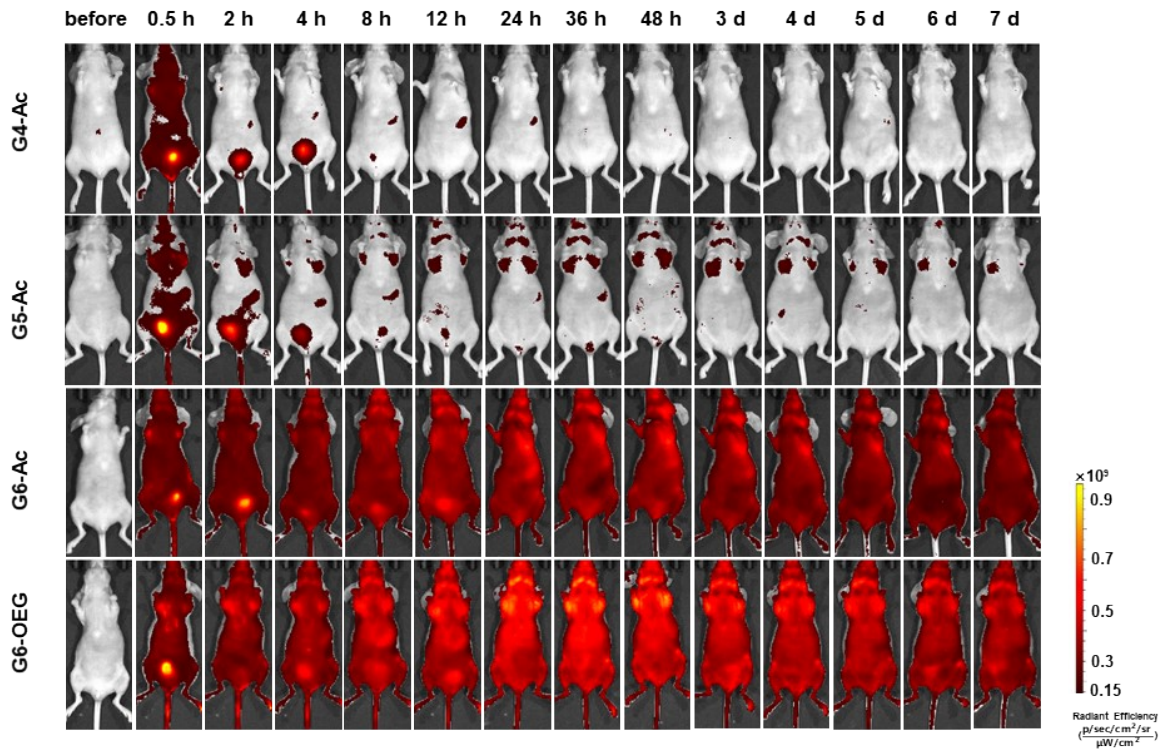

Figure S11. The abdomen fluorescence imaging of the mice with 4T1 breast cancer cells of the PDI-16(DOTA-Gd) PLL dendrimers.

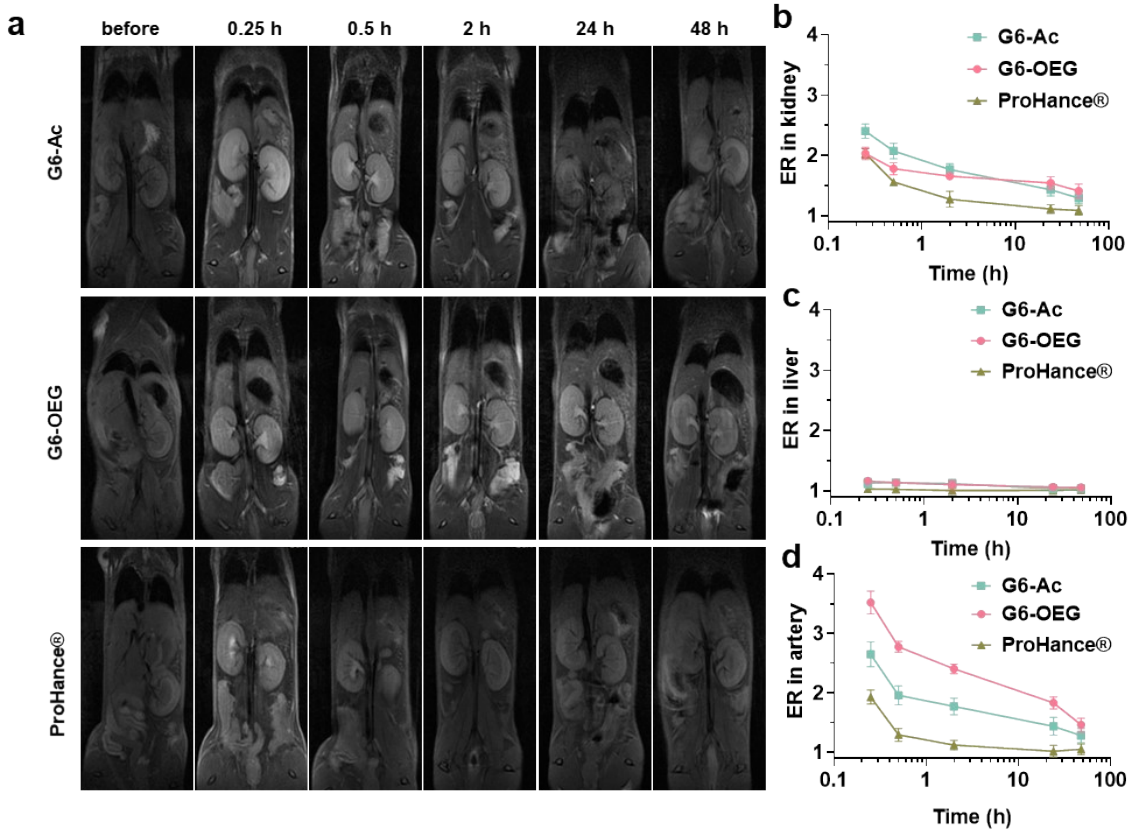

Figure S12. (a) The whole body T1-weighted MR images of mice bearing 4T1 orthotopic tumor before (pre) and after post-injection of ProHance®, G6-Ac and G6-OEG, at 0.1 mmol-Gd/kg. MRI signals enhancement ratio (ER = Spost /Spre) of artery **(b)**, kidneys **(c)** and liver **(d)**.

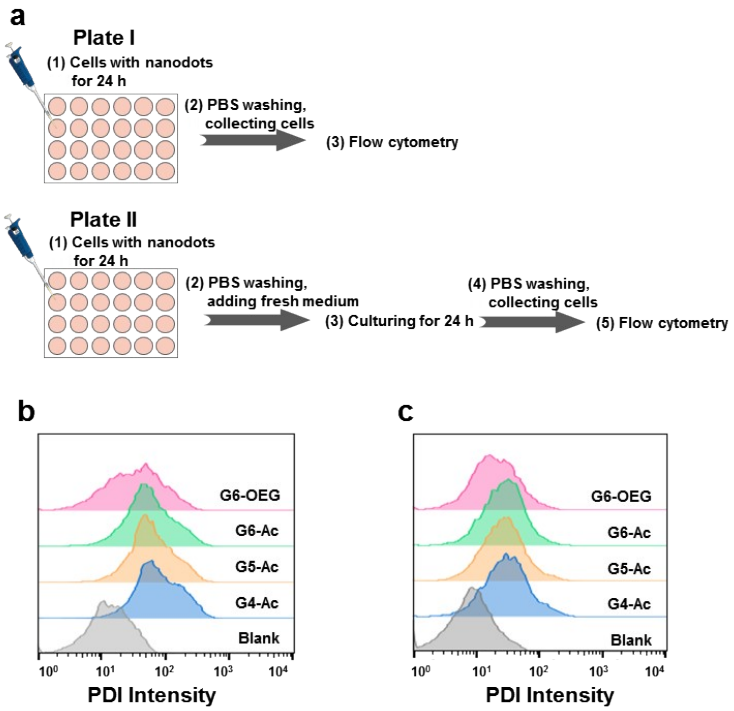

Figure S13. (a) The experimental procedure for determining the cellular take and exocytosis of the nanodots on 4T1 cells. (b) The flow cytometry of 4T1 cells treated with different nanodots (10 μM) for 24 h. (c) The flow cytometry of 4T1 cells with nanodots exocytosed in fresh medium for another 24 h.

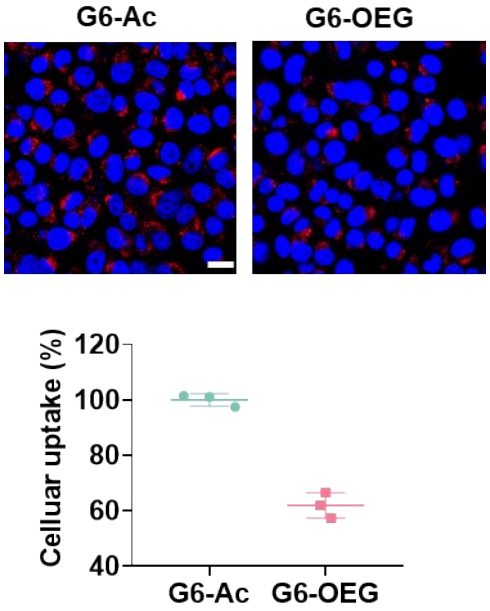

Figure S14. Confocal laser scanning microscopy (CLSM) images and the cellular uptake of 4T1 cells after 12 h incubation with 20 μM of the nanoprobes (Scale bar = 15 μm).

Table S1. Molecular weights of PDI-DOTA PLL dendrimers determined by Maldi-Tof.

Sample	Number of Amines	Theoretical value	Measured by Maldi-Tof
PDI-G2	16	2790.14	2790.71
PDI-16Fmoc-G2.5	16	8390.34	4842.71*
PDI-16DOTA(tBu)-G3	16	13707.13	13707.15
PDI-16DOTA(tBu)-G4	32	15756.65	15757.74
PDI-16DOTA(tBu)-G5	64	19864.69	ND
PDI-16DOTA(tBu)-G6	128	28062.77	ND

Table S2. Molecular weights of PDI-DOTA PLL dendrimers determined by GPC.

Sample	Number of Lysine	Theoretical value	Measured by GPC	PDIs(Mw/Mn)
PDI-G1.5	12	4390	17810	1.09
PDI-16(Fmoc-Boc)-G2.5	28	9991	30390	1.06
PDI-16DOTA(tBu)-G2.5	28	17260	37010	1.08
PDI-16DOTA(tBu)-G3.5	44	22859	38220	1.09
PDI-16DOTA(tBu)-G4.5	76	34059	49910	1.12
PDI-16DOTA(tBu)-G5.5	140	56459	64560	1.14

Table S3. The parameters of the linear fitting in **Figure S6**.

Sample	y = a + b*x			
	Y-intercept (a)	Slope (b)	Pearson's R	R^2 (COD)
ProHance®	0.50 ± 0.05	4.43 ± 0.16	0.99805	0.9961
G4-Ac	0.43 ± 0.22	27.96 ± 0.66	0.99916	0.99832
G5-Ac	0.21 ± 0.49	30.65 ± 1.48	0.99653	0.99308
G6-Ac	0.27 ± 0.12	39.31 ± 0.35	0.99988	0.99976
G6-OEG	0.07 ± 0.12	27.77 ± 0.36	0.99975	0.99949